UC Irvine
UC Irvine Previously Published Works

Title
A Cost-Effective Three-Phase Grid-Connected Inverter with Maximum Power Point Tracking

Permalink
https://escholarship.org/uc/item/0d27f1wr

ISBN
9781424403646

Authors
Chen, Yang
Smedley, Keyue
Brouwer, Jack

Publication Date
2006-10-01

DOI
10.1109/ias.2006.256646

Peer reviewed

A Cost-effective Three-phase Grid-connected Inverter with Maximum Power Point Tracking

Yang Chen[1], Keyue Smedley[1], and Jack Brouwer[2]

1. Dept. of Electrical Engineering and Computer Science
2. National Fuel Cell Center
University of California, Irvine
Irvine, CA 92697, USA
smedley@uci.edu

Abstract—**Solar energy is desirable due to its renewable and pollution-free properties. In order to utilize the present utility grid infrastructure for power transmission and distribution, grid connected dc-to-ac inverters are needed for solar power generation. However, previously proposed voltage source inverters with a two-power-stage structure or a cascaded structure increase the circuit complexity, power losses, and system cost. In addition, conventional maximum power point tracking (MPPT) methods usually need power calculation and complex logic judgment, so expensive multipliers and/or microprocessors are needed. This leads to high inverter capital cost, which becomes a major barrier for the wide use of solar power generation. A cost-effective MPPT method integrated within the One-Cycle Control (OCC) core is proposed in this paper. When integrated with a three-phase boost type inverter, the proposed method tracks MPP with good precision, and solar power is converted into three-phase ac power with a single power stage. There is no power calculation in the controller, which yields a simple and cost-effective solution. Experiments have been carried out with a photovoltaic source to verify good performance.**

Keywords-grid-connected; boost type inverter; One-Cycle Control; maximum power point tracking (MPPT)

I. INTRODUCTION

In recent years, many concerns have been raised regarding fossil fuel-electricity power generation, since it pollutes the environment and depletes limited energy supplies. On the other hand, alternative power sources, such as solar photo-voltaic energy, have gained a lot of attention because they are renewable, friendly to the environment, and flexible for installation. However, these types of sources supply dc power while the present power grid accepts 60Hz ac power, therefore dc-ac grid-connected inverters are necessary for power conversion. To avoid introducing additional distortions to the power grid, the generated currents from these inverters should have low harmonics. Furthermore, when the output currents are in phase with the grid voltages, the maximum active output power is achieved by minimizing the reactive output power. Thus inverters that have high power quality, high efficiency, high reliability, low cost, and simple circuitry are desired.

As far as the alternative source is concerned, each photovoltaic (PV) module or fuel cell stack usually supplies a dc voltage lower than the peak value of the grid voltage, and their output voltages vary in a wide range according to various operating conditions [1]. Series connection of several modules or cells can be a simple way to increase output voltage so as to employ a buck type grid connected inverter [2] for power conversion. However, this method may reduce the overall efficiency [3] because no power will be collected through the inverter when its input dc voltage drops below the peak value of the ac output voltage. There are many publications dedicated to this problem. In article [4] and [5] a two-stage topology that first boosts the dc voltage by a dc-dc converter and then inverts it into ac is used. However, this method increases the complexity of the circuit and losses. In articles [3] and [6] a cascade structure is employed to increase the dc voltage, which needs more power switches and still results in a complex circuit. In article [7], a current source inverter (CSI) employing a large inductor is used for power conversion. However, this type of circuit could be bulky, heavy and expensive for a high power application. In paper [8], a One-Cycle Controlled (OCC) boost-type three-phase grid connected inverter was proposed. It has a single power stage, a low value dc side inductor and its input dc voltage

can vary over a wide range. These key features of OCC are all desirable for low cost high efficiency PV power generation.

As far as maximum power point tracking (MPPT) methods are concerned, many methods have been addressed previously. The Perturb and Observe (P&O) method needs to calculate dP/dV to determine the maximum power point (MPP) [9][10]. Though the method is relatively simple, it can't track the MPP when the irradiance changes rapidly; and it oscillates around the MPP instead of directly tracking it. The Incremental Conductance method tracks MPP rapidly but it has high algorithm complexity, which also employs the calculation of dI/dV [11]. Though this method can accurately determine MPPs, a digital signal processor (DSP) or a microprocessor is usually needed for these complex calculations. The Constant Voltage method [12], which uses 76% open circuit voltage as the MPP voltage, and the Short-Circuit Current method [13] are simple, but they do not always accurately track the real MPP.

In this paper, a cost-effective MPPT method integrated within the OCC controller is proposed. It features the following advantages:

i) *A single power stage*: MPPT and dc-to-ac power conversion can be achieved within a single power stage;

ii) *Simple control circuit*: only the PV output voltage is sensed and used to achieve MPPT; the control circuit preserves the simplicity of OCC method;

iii) *No power calculation and no need for microprocessors or DSPs*: the complexity of the control circuit is greatly reduced;

iv) *Good MPPT capability with acceptable precision*: well tracks the real MPP.

II. REVIEW OF THREE-PHASE BOOST-TYPE GRID-CONNECTED IVERTER [8]

Figure 1 shows the power stage when a PV source is connected to the input side of a boost-type inverter [8], where V_g is the output voltage of the PV array, and meanwhile the input voltage of the inverter; I_g is the output current from the PV and C_{in} is the input dc capacitor of the inverter; L is the dc side inductor. S_{ap}, S_{an}, S_{bp}, S_{bn}, S_{cp} and S_{cn} are six switches in the bridge. Each switch is realized by an IGBT in series with a diode as shown in the dashed line box; and L_{fa}, L_{fb}, L_{fc} and C_a, C_b, C_c are output inductors and capacitors that form an output

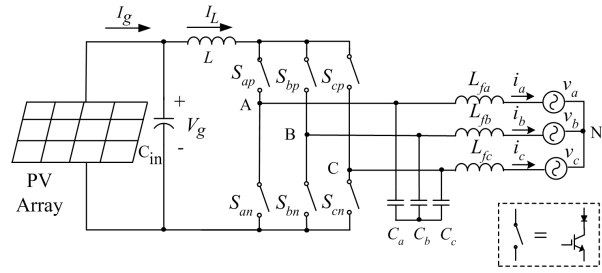filter for the inverter. v_a, v_b and v_c are three-phase grid voltages.

Fig.1 Power stage with PV array connection

Each line cycle can be divided into six regions as shown in Fig.2. For example, in Region I (0~60°), $v_a>0$, $v_c>0$ and $v_b<0$. Additionally, their differential voltages are:

$$v_{ab} \ge \frac{\sqrt{6}}{2}V_{rms} \ , \quad v_{cb} \ge \frac{\sqrt{6}}{2}V_{rms} \tag{1}$$

where, V_{rms} is the rms value of the line-to-neutral voltage.
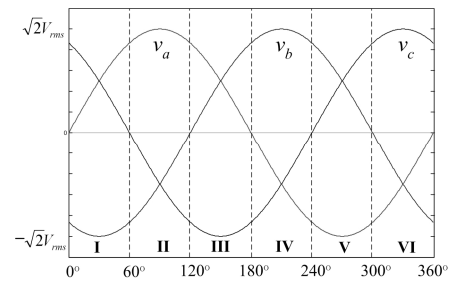

Fig.2 Six regions in a line cycle

Similarly, in other regions two independent phase voltages can always be selected so as to obtain the two differential voltages, which are referred to the third phase voltage, always greater than $\frac{\sqrt{6}}{2}V_{rms}$. Therefore, a boost converter operation is guaranteed as long as the dc voltage V_g satisfies: $V_g \le \frac{\sqrt{6}}{2}V_{rms}$.

At any given instant, one of the upper switches (S_{ap}, S_{bp}, S_{cp}) and one of the lower switches (S_{an}, S_{bn}, S_{cn}) are turned on. For example, in Region I, S_{an} and S_{cn} are kept off and S_{bn} is on for the entire region. S_{ap}, S_{bp} and S_{cp} are controlled at the switching frequency. There are three stages for different switching patterns: 1) Stage I (Fig.3(a)): S_{bp} is turned on and S_{ap}, S_{cp} are off. The inductor current I_L increases, and output currents are supplied by C_a, C_b, C_c; 2) Stage II (Fig.3(b)): S_{ap} is turned on and S_{bp}, S_{cp} are off. I_L decreases through C_a, C_b and v_a, v_b. i_c is supplied by C_c, C_b; 3) Stage III (Fig.3(c)): S_{cp} is turned on and S_{ap}, S_{bp} are off. I_L decreases through C_c, C_b
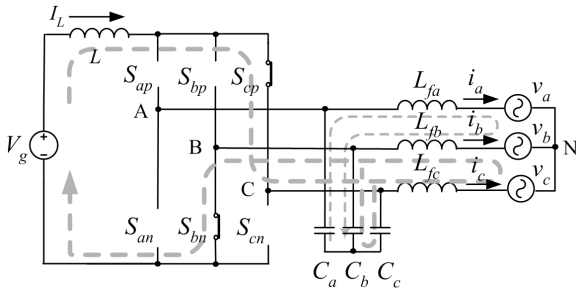
and v_c, v_b. i_a is supplied by C_a, C_b.
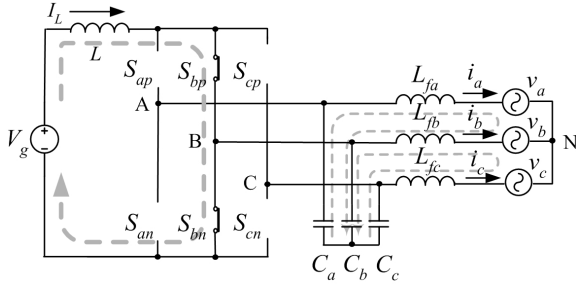
(a) Stage I
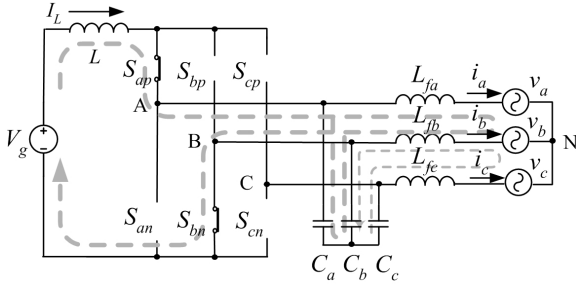
(b) Stage II

(c) Stage III

Fig.3 Three stages for different switching patterns

Figure 4 shows the diagram of OCC core for the boost type inverter. It comprises an integrator with reset, two comparators, two flip-flops and other linear and logic components, where V_{ref} is an adjustable constant and related to output power. R_1 and C_1 are integration components, and $\iota = R_1 C_1 = \dfrac{T_s}{2}$. V_p and V_n are selected from v_a, v_b and v_c in each region respectively; k is the voltage sensing ratio; I_L is the dc side current; and R_s is the current sensing resistance. PWM signal Q_p, Q_n and Q_t are distributed to the corresponding switches for driving IGBTs.

In a balanced three-phase system, the dc side current can be derived as:

$$I_L = \frac{1}{R_s}(V_{ref} - \frac{3k}{2V_g}V_{rms}^2) \tag{2}$$

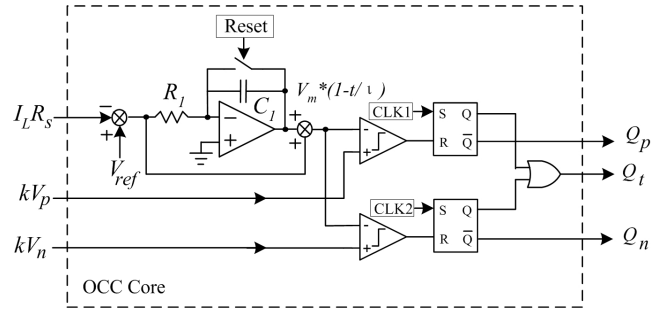Simultaneously, three sinusoidal ac currents can be injected into grids.

Fig.4 Diagram of the OCC core for the boost type inverter

III. CONTROL PRINCIPLE OF MPPT

For a generic PV array that is comprised of M modules in parallel and N cells in series in each module, the output power is:

$$P_g = V_g \cdot I_g = V_g \cdot M \cdot \left\{ I_{LG} - I_{os}[e^{q(V_g+I_g R_{gs})/NAKT} - 1] \right\} \tag{3}$$

where, I_{LG} -- light-generated current of each module;

I_{os} -- reverse saturation current of each module;

q -- electronic charge;

R_{gs} -- series resistance;

A -- ideality factor;

K -- Boltzmann's constant;

T -- temperature in ^oC.

Figure 5 shows the typical output voltage V_g vs. output current I_g curves of a PV source. It can be seen that the MPPs vary with solar irradiance and the cell temperature. When the PV array is connected to the boost inverter, the actual operation point of the PV source is determined by the external circuit as well as the solar irradiance and cell temperature at
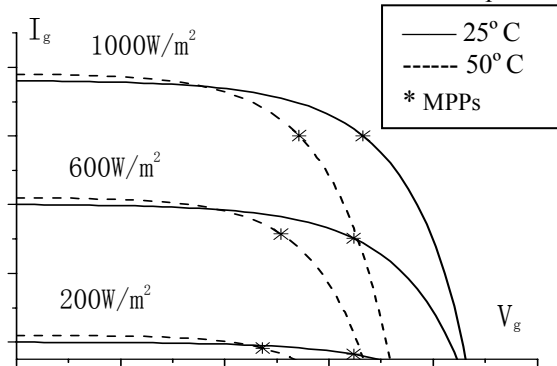

Fig. 5 V_g~I_g curves of a PV source

any instant. In order to extract the maximum power from the PV array, the boost inverter should: i) allow input voltage to vary in a large range; ii) make input power track the MPP for different operating circumstances (e.g., temperature, irradiance).

From the analysis in [8], the boost inverter allows input voltage to change as long as $V_g \leq \frac{\sqrt{6}}{2} V_{rms}$ is satisfied. The input power of the inverter can then be derived from (2):

$$P_{in} = V_g \cdot I_L = \frac{1}{R_S}(V_g \cdot V_{ref} - \frac{3k}{2} V_{rms}^2) \qquad (4)$$

In order to make P_{in} approach MPPs automatically, a cost-effective MPPT method is proposed in this paper. Figure 6 shows the diagram of the controller with the MPPT function integrated in the OCC core. Only V_{ref} (in Fig.4) is replaced by $k_g V_g$ in order to achieve a better MPPT tracking capability. k_g is the voltage sensing ratio and V_g is the output voltage of the PV array. Thus:
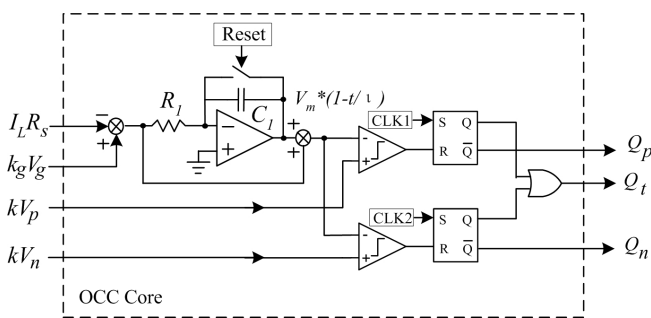
$$V_{ref} = k_g V_g \qquad (5)$$

Fig.6 OCC controller with MPPT function

Substituting (5) into (4), the following can be obtained:

$$P_{in} = \frac{1}{R_S}(k_g V_g^2 - \frac{3k}{2} V_{rms}^2) \qquad (7)$$

Since R_s, k_g and k are constant for any particular circuit design and V_{rms} is fixed, the input power of the inverter P_{in} is only related to its input voltage V_g. With the help of Matlab simulation of the proposed circuit design, the output power P_g of the PV and the input power P_{in} of the inverter can be drawn as shown in Fig.7, where the solid lines indicate P_g vs. V_g at three different solar irradiance levels (as shown in Fig.5) at 25ºC, and the dashed lines are the corresponding curves at 50ºC. The P_{in} curve is superimposed onto the same graph

versus V_g in Fig.7. At any time, when the input power of the inverter equals the output power of the PV, a temporary steady state of the system is achieved. These steady state operating conditions are represented by a series of intersection points between P_{in} and P_g in Fig.7. These intersection points are the desired operating points for the circuit proposed in this paper. When solar irradiance or temperature changes, the operation point can move up or down along the P_{in} curve to satisfy the condition $P_{in}=P_g$. By this means, the inverter can adjust its input power automatically according to the variation of P_g caused by operating circumstances. For any particular application case in which the output properties of the PV source are known, parameters R_s, k_g and k in (7) can be tuned to make the P_{in} curve closely approach the MPPs. Thus, the MPPT function is achieved with an acceptable precision.
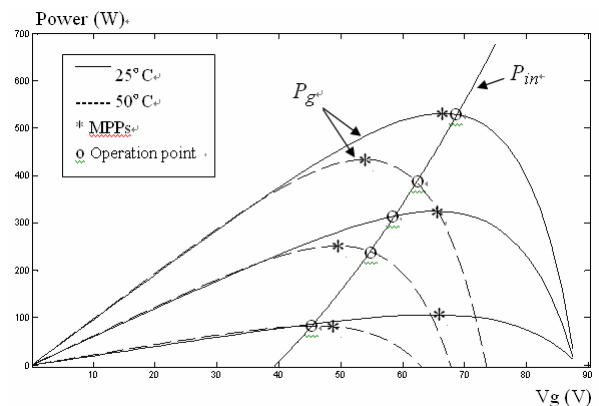

Fig.7   Simulation results for P_g and P_{in} versus V_g

IV.   EXPERIMENTAL VERIFICATION

Experiments have been conducted with the proposed MPPT method using a PV array consisting of 8 modules that are divided into two groups. Each group comprises four series-connected modules and then these two groups are parallel-connected. The PV array was installed on the rooftop of the Engineering Laboratory Facility at University of California, Irvine with a 60º angle of incidence and facing roughly 45º east of due south. The specifications of each panel are as follows:

Model type: Shell SP75;

Peak power: 75W (the peak power is achieved with direct irradiance levels of 1000W/m^2 of spectrum AM 1.5 when the cells are at 25ºC);

Short circuit current: 4.8A;

Open circuit voltage: 21.7V;

Other key parameters of the system are:

CLK1 and CLK2 frequency: $f_s = 40$ kHz;

DC side capacitor: $C = 3$mF;

DC side inductor $L = 0.6$mH;

$k_g = 0.0675$; $R_s = 0.332\Omega$; k = 0.0096;

Figure 8 presents the experimental observations. The upper two curves show the output power P_g and the actual maximum power P_{max} of the PV during the daytime (All the data of Fig.8 are based on the experiments conducted on Aug. 26th, 2005, in Irvine CA. Weather conditions were sunny, 65-91 ^{o}F, humidity of ~50%, and winds generally SSW at 6 mph.). The bottom bar chart shows the relative error between P_g and P_{max}. The achieved power curve closely matches maximum power throughout the period. When P_{max} hits its peak around 13:00 the relative error is only 3.8%. However, before 10:00 and after 16:00 when the temperature drops significantly from that of midday, the error increases up to almost 20%, because the proposed MPPT method does not account for temperature variations. Nonetheless, the proposed the MPPT method closely tracks MPPs (especially during the period of peak output) with an acceptable precision. In addition, the experimental results well match those predicted by the Matlab simulation.
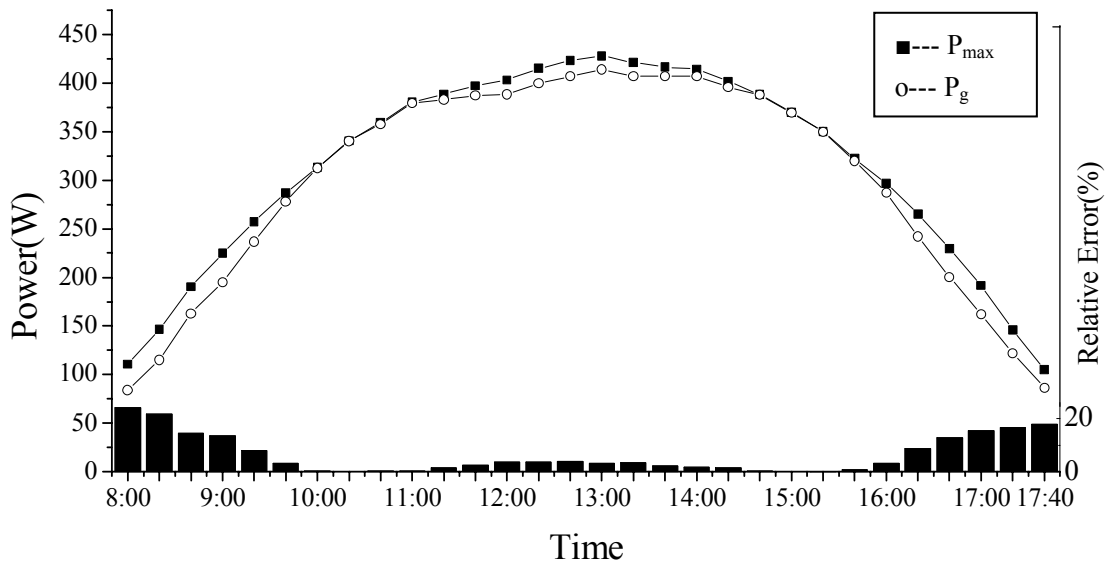

Fig.8 The extracted power P_g, the maximum P_{max} and relative error vs. time

Figures 9 and 10 present typical voltage and current waveforms acquired during the experiments. Since the total output power of the PV is small, the output voltage of the inverter is reduced to half of the nominal phase voltage in order to get better three-phase current waveforms. Figure 9 shows the input voltage and current of the inverter. The dc side current is kept almost constant by the proposed control method. The current ripple in the line cycle frequency range is caused by the unbalanced situation of the three-phase system. Figure 10 shows phase A voltage and three output currents of the inverter. The currents are approximately sinusoidal and follow the corresponding phase voltages respectively. Thus, a near unity power factor can be achieved. The THD of the current is approximately 3.5%.

V. CONCLUSIONS

In this paper, a cost-effective MPPT method is proposed for the three-phase boost-type grid-connected inverter. The control method is simple and can be integrated within the OCC core by adding a few simple components. Complex power calculation is not needed, and multipliers or
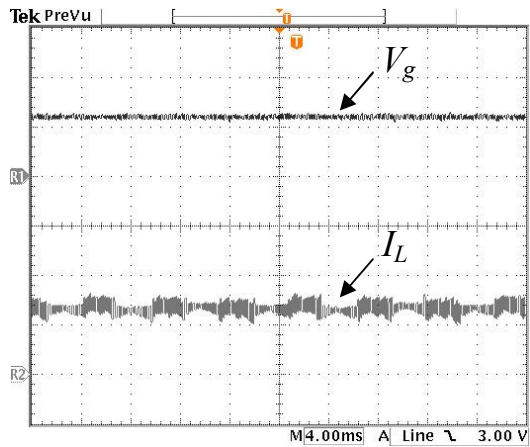
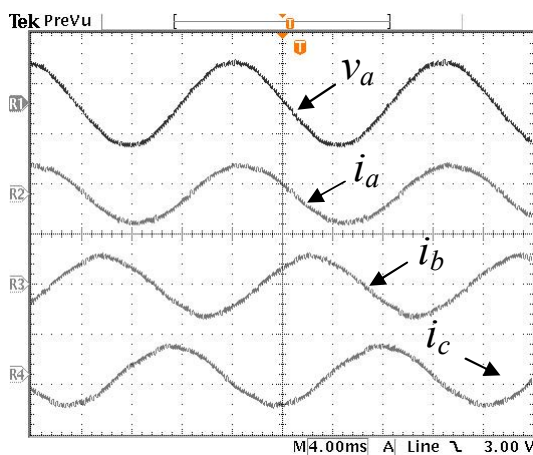Fig.9 Input of the inverter V_g (50V/div), I_L (5A/div)

Fig.10 Output of the inverter: v_a (100V/div),

i_a, i_b, i_c (5A/div)

microprocessors are not necessary. The proposed circuit requires only one power stage to achieve the MPPT function and dc-to-ac power conversion, which makes the whole system simple and cost-effective. Experiments were conducted using one embodiment of the proposed design as applied to a photovoltaic source. Data shows that the proposed method has good MPPT capability and high quality output performance, and it is a good candidate for use in solar power generation.

REFERENCES

[1] G.K. Andersen, C. Klumpner, S.B. Kjaer, F. Blaabjerg, "A new green power inverter for fuel cells", Power Electronics Specialists Conference, 2002. pesc 02. 2002 IEEE 33rd Annual, Volume 2, 23-27 June 2002 Page(s):727 - 733 vol.2

[2] C. Qiao, K.M. Smedley, "Three-phase grid-connected inverters interface for alternative energy sources with unified constant-frequency integration control", Industry Applications Conference, 2001. Thirty-Sixth IAS Annual Meeting. Conference Record of the 2001 IEEE Volume 4, 30

Sept.-4 Oct. 2001 Page(s):2675 - 2682 vol.4

[3] G.R. Walker, P.C. Sernia, "Cascaded DC-DC converter connection of photovoltaic modules", Power Electronics, IEEE Transactions on, Volume 19, Issue 4, July 2004 Page(s):1130 – 1139

[4] F. Antunes, A.M. Torres, "A three-phase grid-connected PV system", Industrial Electronics Society, 2000. IECON 2000. 26th Annual Conjerence of the IEEE Volume 1, 22-28 Oct. 2000 pp. 723 - 728 vol.1

[5] J.C. Lima, J.M. Corleta, A. Medeiros, V.M. Canalli, F. Antunes, F.B. Libano, F.S. Dos Reis, "A PIC controller for grid connected PV system using a FPGA based inverter", Industrial Electronics, 2000. ISIE 2000. Proceedings of the 2000 IEEE International Symposium on Volume 1, 4-8 Dec. 2000 Page(s):169 - 173 vol.1

[6] M. Calais, V.G. Agelidis, L.J. Borle, M.S. Dymond, "A transformerless five level cascaded inverter based single phase photovoltaic system", Power Electronics Specialists Conference, 2000. PESC 00. 2000 IEEE 31st Annual Volume 3, 18-23 June 2000 Page(s):1173 - 1178 vol.3

[7] J.S. Siva Prasad, B.G. Fernandes, "Active commutated thyristor CSI for grid connected photovoltaic applications", Power Electronics and Motion Control Conference, 2004. IPEMC 2004. The 4th International, Volume 3, 14-16 Aug. 2004 Page(s):1767 - 1771 Vol.3

[8] Y. Chen, K. Smedley, "Three-Phase Boost Type Grid Connected Inverter", Applied Power Electronics Conference and Exposition, 2006, Mar. 19-23

[9] O. Wasynczuk, "Dynamic behavior of a class of photovoltaic power systems," IEEE Trans. Power App. Syst., vol. PAS-102, pp.3031–3037, Sept. 1983

[10] E. Koutroulis, K. Kalaitzakis, N.C. Voulgaris, "Development of a Microcontroller-Based, Photovoltaic Maximum Power Point Tracking Control System", IEEE Transactions on Power Electronics, Vol.16, No.1, pp.46-54, January 2001

[11] K.H. Hussein, I. Muta, "Maximum Photovoltaic Power Tracking: An Algorithm for Rapidly Changing Atmospheric Conditions", IEEE Proceedings on Generation, Transmission, and Distribution., Vol.142, No.1, pp.59-64, January 1995

[12] T. Noguchi, S. Togashi, R.Nakamoto, "Short-Current Pulse-Based Adaptive Maximum-Power-Point Tracking for a Photovoltaic Power Generation System", Electrical Engineering in Japan, Vol.139, No.1, pp65-72, 2002[Denki Gakkai Ronbunshi, Vol.121-D, No.1, pp.78-83, January 2001]

[13] J.H.R. Enslin, M.S. Wolf, D.B. Snyman, W. Swiegers, "Integrated Photovoltaic Maximum Power Point Tracking Converter", IEEE Transactions on Industrial Electronics, Vol.44, No.6, pp.769-773, December 1997

[14] Y. Chen, K. Smedley, "Three-Phase Boost Type Grid-Connected Inverter", US and International Patent Application.